Available online at www.sciencedirect.com

ScienceDirect

Procedia Engineering 102 (2015) 1599 – 1611

Procedia Engineering

www.elsevier.com/locate/procedia

The 7th World Congress on Particle Technology (WCPT7)

A CFD Simulation of 3D Air Flow and Temperature Variation in Refrigeration Cabinet

Limin Wang[a,*], Lin Zhang[a], Guoping Lian[b,c]

[a]*State Key Laboratory of Multiphase Complex Systems, Institute of Process Engineering, Chinese Academy of Sciences, Beijing 100190, China.*
[b]*Unilever R&D Colworth, Sharnbrook, Bedford MK44 1LQ, UK.*
[c]*Department of Chemical and Process Engineering, University of Surrey, Guildford GU2 7XH, UK.*

Abstract

Presented is a 3D simulation of the air flow and temperature variation in an ice drink refrigeration cabinet, during an automated dynamic cycle of switching on and switching off. To correctly model the effect of perforated plate separating evaporator and storage compartments, a benchmark problem is designed, and used as a reference to determine the parameters in the porous-jump model by parameter optimization. Subsequently, the dynamic cycle of initial switch on, automated switch off and automated switch on is simulated. Both the flow field distribution and temperature profile are analyzed and the time required for these three stages is obtained. Full 3D CFD simulation of refrigeration system provides not only detailed temperature distribution in the cabinet but also operational parameters of the system such as for switch on-off cycle. Those output from simulation are important for cabinet design to improve the storage quality of products while reducing the energy use.

Selection and peer-review under responsibility of Chinese Society of Particuology, Institute of Process Engineering, Chinese Academy of Sciences (CAS)

Keywords: Refrigeration cabinet; CFD; Dynamic cycle; Perforated plate

* Corresponding author. Tel.: +8-610-825-44942; fax: +8-610-625-58065.
E-mail address: lmwang@ ipe.ac.cn

Selection and peer-review under responsibility of Chinese Society of Particuology, Institute of Process Engineering, Chinese Academy of Sciences (CAS)
doi:10.1016/j.proeng.2015.01.296

1. Introduction

Many food products sold through supermarkets, grocery stores and small outlets require refrigeration. Generally, refrigeration cabinet is designed to keep foods at specific temperature to ensure optimal freshness, quality, safety and shelf life. A major concern on food refrigeration is the high energy consumption. It is reported that a typical supermarket in the UK uses approximately 1000 kWh m^{-2} energy, of which about 40% to 50% is consumed for refrigeration purposes [1]. Indeed, refrigeration is regarded as a significant contributor for carbon emission, and also impacts on environment due to large quantity of refrigerant discharges [2]. There is a great need to better design refrigeration cabinet, despite of improvements made in the last 20 years.

From the viewpoint of heat transfer, a refrigeration cabinet is composed of three main components, namely the cabinet cavity, the insulation and the refrigerating unit. The refrigerating system controls the temperature of products by circulating cold air around and removing the heat ingression from cabinet wall and display [3]. Many factors affect refrigeration cabinet operation. A thorough comprehension of the dynamic air circulation and heat transfer in refrigeration cabinet is highly required but it is a very challenging task. Experimental tests are hugely time consuming and capital intensive, and can be carried out only for simple components [4-8]. Computational fluid dynamics (CFD) modelling would be a viable choice, which can reduce experiments [9]. Many studies have shown that CFD modelling is a promising and valuable tool to improve refrigeration efficiency in terms of energy savings and the required temperature maintenance. Foster et al. [10] used CFD to simulate a chilled multi-deck retail display cabinet. Cortella [11] employed CFD to predict the air flow pattern and food temperature inside cabinet. Based on the stream function-vorticity formulation, Cortella et al. [12] adopted finite element method to analyze the flow velocity and temperature distribution of air in an open display refrigeration cabinet. Resorting to a modified two-fluid model and an adaptive support vector machine algorithm, Cao et al. [13] proposed a novel strategy for predicting air flow and temperature profile in an open vertical display refrigeration cabinet. A review by Smale et al. [14] highlighted the complementary role of CFD analysis to experimental studies, and demonstrated the ability of CFD to capture the critical domains of temperature occurring in the front of the stock.

Most CFD modelling studies reported in the literatures are limited to 2D, either with commercial codes or with in-house codes. It has been recognized that cabinet performance in 3D is very different from 2D simulations [15]. For example, air flow visualization performed on air curtain of open display cabinet showed that 3D effects can be significant, even with still air in the ambient, not to mention the varying ambient air flow. Most reported CFD simulations are also limited to steady-state air flow and temperature distribution of cabinet. Integrated numerical simulation of the dynamic operation of whole refrigeration systems including both cabinet and refrigerator still remains a challenging task. In this paper, we report the progress in 3D simulation of a full refrigeration cabinet system under dynamic operation of automated switching on and switching off. The system is an enclosed display cabinet for ice drink products, where strict product temperature range is required. In order to achieve integrated simulation of the cabinet system with realistic refrigeration, sub-models for modelling coolant air generation (refrigeration) and distribution through perforated plate have been proposed and discussed. The aim is to present an improved CFD simulation of refrigeration cabinet systems under realistic air flow, heat transfer and dynamic operation conditions.

2. CFD model of refrigeration cabinet

2.1 Description of the refrigeration cabinet

The refrigeration cabinet is schematically shown in Fig.1. It is a horizontal open-top display unit for frozen drink products requiring storage temperature between -5ºC and -7ºC. The evaporation tube of refrigeration is at the back and enclosed by a plastic plate, preventing the cavity for storing products from getting too cold. The enclosing plate is perforated at the top and bottom to allow coolant air to circulate. A propeller fan is installed in the coolant air chamber near the perforated plate to assist air circulation.

The main design parameters of the refrigeration cabinet are outlined below:

- The depth, width and height of the refrigeration cabinet cavity including the chamber for enclosing the evaporation tube are 587mm, 440mm, 632mm respectively.

- The thickness of the enclosing plate is 3mm and the thickness of the insulation walls (polyurethane) is 80mm.
- The glass door with thickness of 8mm consists of two parts; one is 282mm fixed at the back, and the other the sliding glass door of 305mm at the front.
- The depth of the refrigeration room is 707mm.
- The enclosing plate is perforated near the top with 75mm, and has an open channel of 90mm.

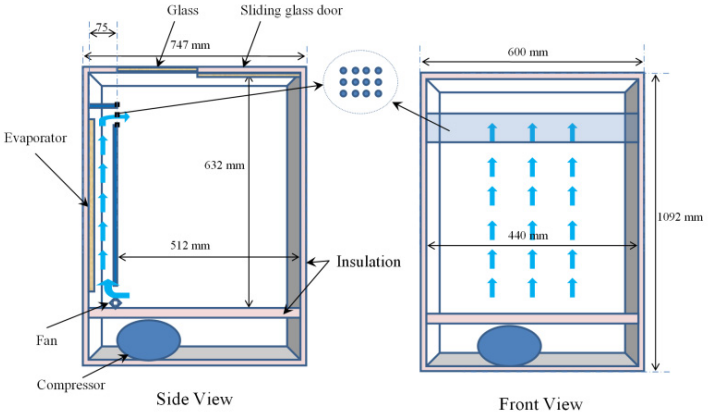

Fig 1 The sketch of the simulated refrigeration cabinet

2.2 Modelling perforated plate

Fig. 2 presents the CFD simulation box of the refrigeration cabinet, in which the perforated plate is used to distribute coolant air into the display cabinet to ensure uniform temperature of the frozen drink. The perforated plate will be modelled by the porous-jump model. The reason is that this simple model is more robust and yields better convergence. It was recommended to be used whenever possible over the full porous media model.

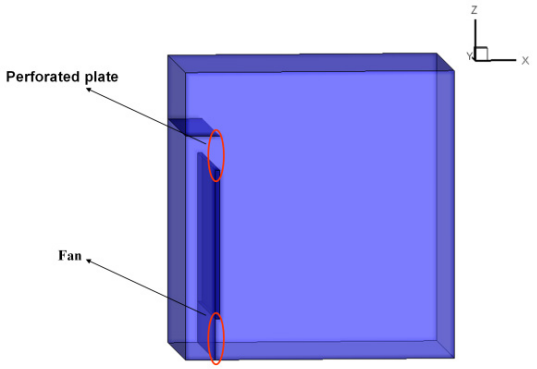

Fig 2 CFD simulation box of the refrigeration cabinet

With the porous-jump model, the thin perforated plate is modelled as a porous medium of finite thickness. The pressure drop is from a combination of Darcy's law and an additional inertial loss term:

$$\Delta p = -\left(\frac{\mu}{\alpha} v + C_2 \frac{1}{2} \rho v^2 \right) \Delta m \tag{1}$$

where C_2 is the pressure-jump coefficient, v is the velocity normal to the porous plate, and Δm is the thickness of the

plate.

For the perforated plate, the Darcy's pressure drop is negligibly small and can be eliminated with only the inertial loss term retained, yielding the following simplified form.

$$\Delta p = -C_2 \frac{1}{2} \rho v^2 \Delta m \tag{2}$$

2.3 Air flow and heat transfer equations

Air within the cabinet is modelled as an ideal gas. The governing equations for air flow and heat transfer are listed as follows:

Mass conservation equation:

$$\frac{\partial \rho}{\partial t} + \frac{\partial}{\partial x_j}\left(\rho U_j\right) = 0 \tag{3}$$

Momentum conservation equation:

$$\frac{\partial}{\partial t}\left(\rho U_i\right) + \frac{\partial}{\partial x_j}\left(\rho U_i U_j\right) = -\frac{\partial p}{\partial x_i} + \frac{\partial}{\partial x_j}\left(\tau_{ij} - \rho\overline{u_i u_j}\right) + S_M \tag{4}$$

Energy conservation equation:

$$\frac{\partial}{\partial t}\left(\rho h_{tot}\right) - \frac{\partial p}{\partial t} + \frac{\partial}{\partial x_j}\left(\rho U_j h_{tot}\right) = \frac{\partial}{\partial x_j}\left(\lambda \frac{\partial T}{\partial x_j} - \rho\overline{u_j h}\right) + \frac{\partial}{\partial x_j}\left(U_i\left(\tau_{ij} - \rho\overline{u_i u_j}\right)\right) + S_E \tag{5}$$

where τ_{ij} is the molecular stress tensor, $-\rho\overline{u_i u_j}$ is the Reynolds stresses, $-\rho\overline{u_j h}$ is an additional turbulence flux term. Here,

$$\tau_{ij} = \mu\left(\frac{\partial U_i}{\partial x_j} + \frac{\partial U_j}{\partial x_i}\right) - \frac{2}{3}\mu \frac{\partial U_i}{\partial x_i}\delta_{ij} \tag{6}$$

$$-\rho\overline{u_i u_j} = \mu_t\left(\frac{\partial U_i}{\partial x_j} + \frac{\partial U_j}{\partial x_i}\right) - \frac{2}{3}\left(\rho k + \mu_t \frac{\partial U_i}{\partial x_i}\right)\delta_{ij} \tag{7}$$

$$-\rho\overline{u_j h} = \frac{\mu_t}{Pr_t}\frac{\partial h}{\partial x_j} \tag{8}$$

in which h is the static enthalpy and $\mu_t = C_\mu \rho k^2/\varepsilon$.

The values of k and ε come directly from the differential transport equations for the turbulence kinetic energy and turbulence dissipation rate. For standard $k-\varepsilon$ model, the transport equations have the following forms:

Turbulence kinetic energy equation:

$$\frac{\partial}{\partial t}(\rho k)+\frac{\partial}{\partial x_i}(\rho U_i k)=\frac{\partial}{\partial x_j}\left(\left(\mu+\frac{\mu_t}{\sigma_k}\right)\frac{\partial k}{\partial x_j}\right)+G_k+G_b-\rho\varepsilon-Y_M+S_k \tag{9}$$

Turbulence dissipation rate equation:

$$\frac{\partial}{\partial t}(\rho\varepsilon)+\frac{\partial}{\partial x_i}(\rho U_i\varepsilon)=\frac{\partial}{\partial x_j}\left(\left(\mu+\frac{\mu_t}{\sigma_\varepsilon}\right)\frac{\partial \varepsilon}{\partial x_j}\right)+C_{\varepsilon 1}\frac{\varepsilon}{k}(G_k+C_{\varepsilon 3}G_b)-C_{\varepsilon 2}\rho\frac{\varepsilon^2}{k}+S_\varepsilon \tag{10}$$

where G_k represents the generation of turbulence kinetic energy due to the mean velocity gradient, G_b is the generation of turbulence kinetic energy due to buoyancy, Y_M represents the contribution of the fluctuating dilatation in compressible turbulence to the overall dissipation rate, σ_k and σ_ε are the turbulent Prandtl numbers for k and ε respectively.

For an ideal gas, the density is calculated from the ideal gas law and c_p is (at most) a function of temperature: $p=wp_{abs}/R_0T$, $\mathrm{d}h=c_p\mathrm{d}T$ and $c_p=c_p(T)$ where w is the molecular weight, p_{abs} is the absolute pressure and R_0 is the universal gas constant.

2.4 Boundary conditions and equation solver

The pressure drop of the fan "EBMPAPST 9956M" for air circulation is obtained from its performance curve (i.e. the P-Q curve of fan), then we have

$$\begin{aligned}\Delta p_{fan}&=31.62566+30.56635v-905.66131v^2+3154.58318v^3\\&\quad-4300.86952v^4+2226.95294v^5-255.42003v^6\end{aligned} \tag{11}$$

where Δp_{fan} is the pressure drop caused by fan, and v is the velocity of air normal to the entry face. All the cabinet walls are set to be a no-slip condition for velocity. As for heat flux, the conductive boundary condition is applied where the heat flux is calculated from the temperature difference between the inside wall and the ambient reference, with the heat transfer coefficient of 6 W K^{-1} m^{-2} for the glass door and that of 0.2625 W K^{-1} m^{-2} for the insulation wall. The value of 0.2625 W K^{-1} m^{-2} comes from the thickness of the insulation wall 80mm and its thermal conductivity 0.021 W K^{-1} m^{-1}. (Specially, when the evaporator is switched on the corresponding wall is set as a constant temperature boundary condition with –23.3°C, while when the evaporator is switched off the corresponding wall is set as the convective boundary condition with heat transfer coefficient 0.2625 W K^{-1} m^{-2}. Here, the value of –23.3°C is the evaporating temperature of refrigerant, in order to agree with the cooling capacity of the compressor used. Finally, the adiabatic boundary condition is applied at the left walls including both the separated plate and the upper wall of the refrigeration room).

The software GAMBIT is used to build up the geometry model of the constructed component. Smooth transition is introduced at the junctions. Structured hexahedral regular elements are applied for meshing. The commercial code FLUENT is employed as the equation solver to solve the governing equations. The SIMPLE algorithm is selected to compute the velocity, pressure and temperature, and the calculations are performed in single precision.

3. Parameter optimization

As mentioned above, in order to consider the effect of perforated plate, the porous-jump model is used in which

there is an unknown parameter C_2. Here a benchmark problem is proposed as a reference to determine this parameter. Subsequently, in FLUENT we set the perforated plate area as fluid type and choose the porous zone option to set the determined parameter.

2.1 Benchmark problem

The proposed benchmark problem is with one open channel whose area is equivalent to the total effective open area of the holes of the perforated plate. By matching the overall flux of porous flow, the parameter C_2 is determined.

Fig 3(a) and Fig 3(b) present the constructed component and its meshing respectively, in which the open channel is located in the top right corner of the cavity and its area is 1/4 times that of the perforated plate, namely the height is 18.75mm. In the refrigeration compartment, the mesh is much finer than that in the storage compartment, because its velocity and temperature fluctuations are very fast.

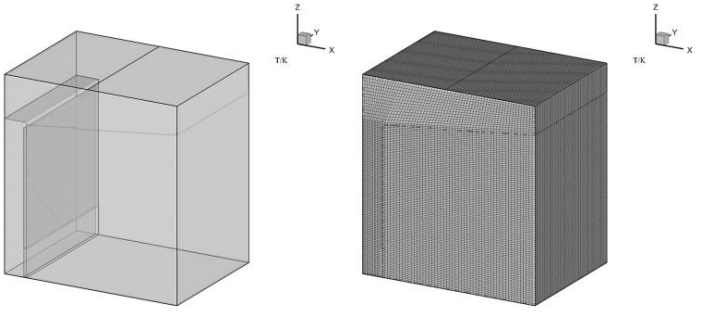

(a) (b)

Fig 3 The constructed component (a) and its meshing (b)

Fig 4(a) and Fig 4(b) present the flow field and temperature distribution of the benchmark problem at the cross section of *y*=220mm respectively. From Fig 4(a) we can see that: (1) most of region in the refrigeration room is of high velocity; (2) in the storage compartment, the highest velocity is about 1.0 m s^{-1} which appears near the open channel; (3) most region in the storage compartment is of lower velocity, except the region near the open channel. From Fig 4(b) we can see that: (1) almost half region in the refrigeration room has the same temperature as that in most storage room, and the left region near the evaporator has the lowest temperature; (2) the fluid passing through the open channel has a relatively low temperature; (3) most region in the storage room is of the same low temperature, and the highest temperature appears to be near the front of the glass door.

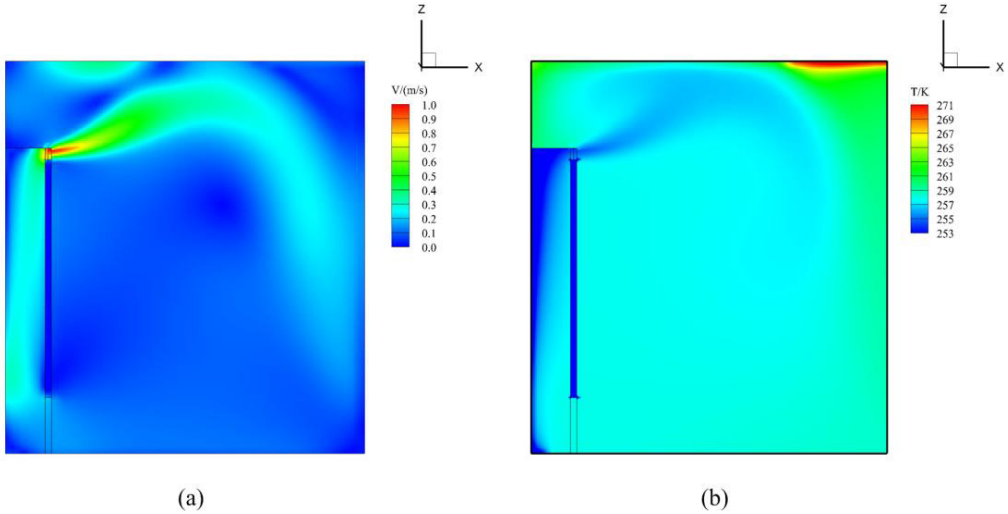

Fig 4 The flow field (a) and temperature distribution (b) of benchmark problem

Finally, it should be pointed out that the mass flow rate across the open channel equals to 0.0088022165 kg s^{-1}. This value will be used as a reference to optimize the parameter C_2.

2.2 Optimization of C_2 in the porous-jump model

Fig 5 presents the optimization procedure of the pressure-jump coefficient C_2 in the porous-jump model. Here the governing equations are also steady. Similarly, we assign different values to C_2 to calculate the mass flow rate across the upper perforated plate. When $C_2 = 2900.725$, the corresponding mass flow rate is 0.0087795546 kg s^{-1}, which is very close to 0.0088022165 kg s^{-1}. So $C_2 = 2510.017$ is adopted in the porous-jump model to study the flow in the refrigeration cabinet.

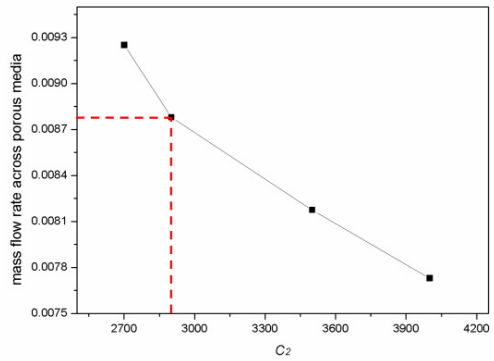

Fig 5 The optimization of the pressure-jump coefficient C_2 in the porous-jump model

4. Dynamic cycle of refrigeration cabinet in 3D

Food requires strict temperature control. For the particular application of ice drink product, the required temperature is between - 7℃～ - 5℃. When refrigeration cabinet is switched on, air in the storage compartment is

cooled from room temperature (i.e. 25℃) to the lower setting of the required temperature (- 7℃ in this case). With build-in auto-control system, the refrigerator will cut off once the lower setting of temperature is reached. However, heat ingression from external environment occurs continually and will eventually lead to temperature rise in the cabinet. When the temperature in the cabinet rises to the upper limit of the required temperature, i.e. - 5℃ in this case, the built-in auto-control system will automatically turn on the refrigerator. The next cycle of cooling starts. Here we simulate these three stages of refrigeration by CFD simulation in 3D: (1) the stage from room temperature to - 7℃ (cooling switched on firstly); (2) the stage from - 7℃ to - 5℃ (cooling switched off subsequently); (3) the stage from - 5℃ to - 7℃ (cooling switched on again). Meanwhile, we predict an important parameter of control, namely the needed time of each stage. Here, a temperature sensor is fixed on the wall of (587mm, 220mm and 492mm) to detect the temperature of the storage cabinet.

2.1 Stage from room temperature to - 7℃

Fig 6 presents the evolution of flow field from room temperature to - 7℃. Initially, the fluid in refrigeration cabinet is stationary, namely the magnitude of velocity equals to zero. Then, under the action of fan, air begins to flow mainly in refrigeration room. With time goes on, the air flows to pass through the upper perforated plate and leads to the air in storage room to flow. We can observe that the highest velocity occurs near the fan in the refrigeration compartment and increases with time until the flow is fully developed.

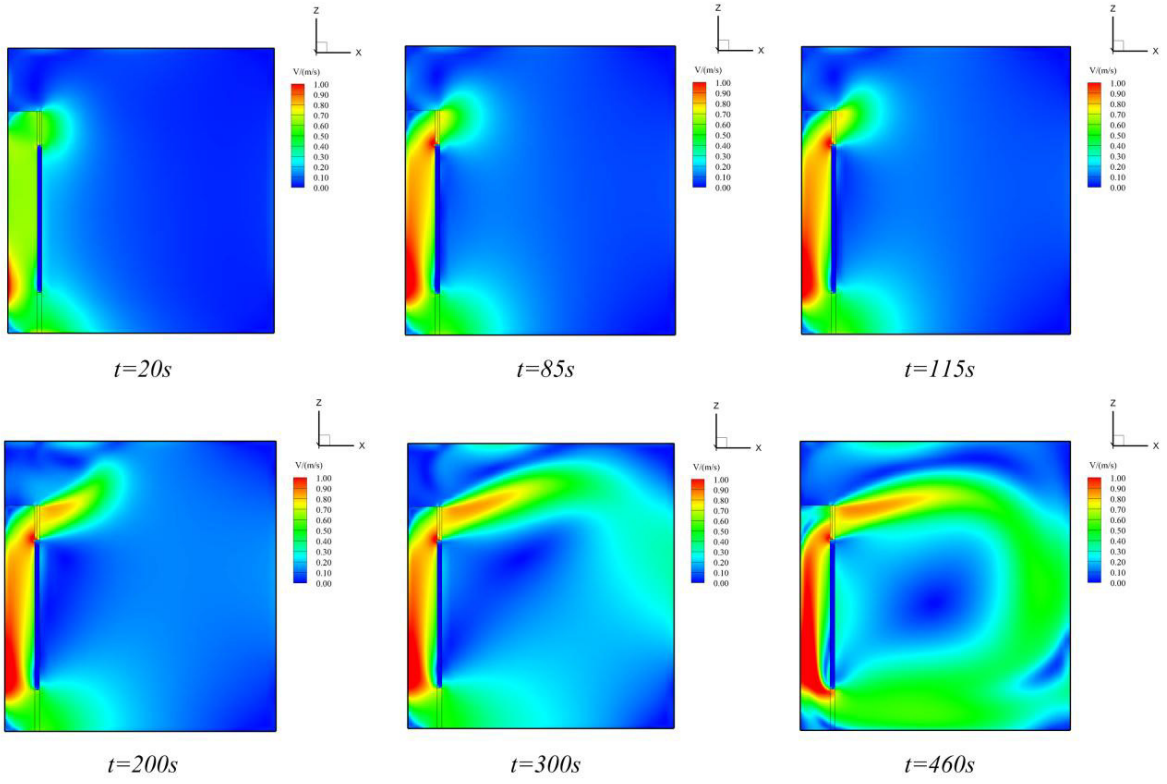

Fig 6 The evolution of flow field from room temperature to - 7℃

Fig 7 presents the evolution of temperature distribution from room temperature to - 7℃. At the initial time, all air in the refrigeration cabinet is set to be room temperature. After the refrigeration is switched on, the air in refrigeration room is cooled. The temperature near the evaporator is lower than that near the opposite side, and there is an obvious temperature gradient appeared in refrigeration room. Meanwhile, under the action of fan, the cooled

air flows into the storage room from the upper perforated plate. Near to the back of the glass door, there is a zone with relatively high temperature. This is a recirculating zone less affected by the cooled air flow. Finally, it can be observed obviously that almost all the region in the storage room is cooled at －7℃, and the time cooled from room temperature to －7℃ is about 460s (see t=460s in Fig 7).

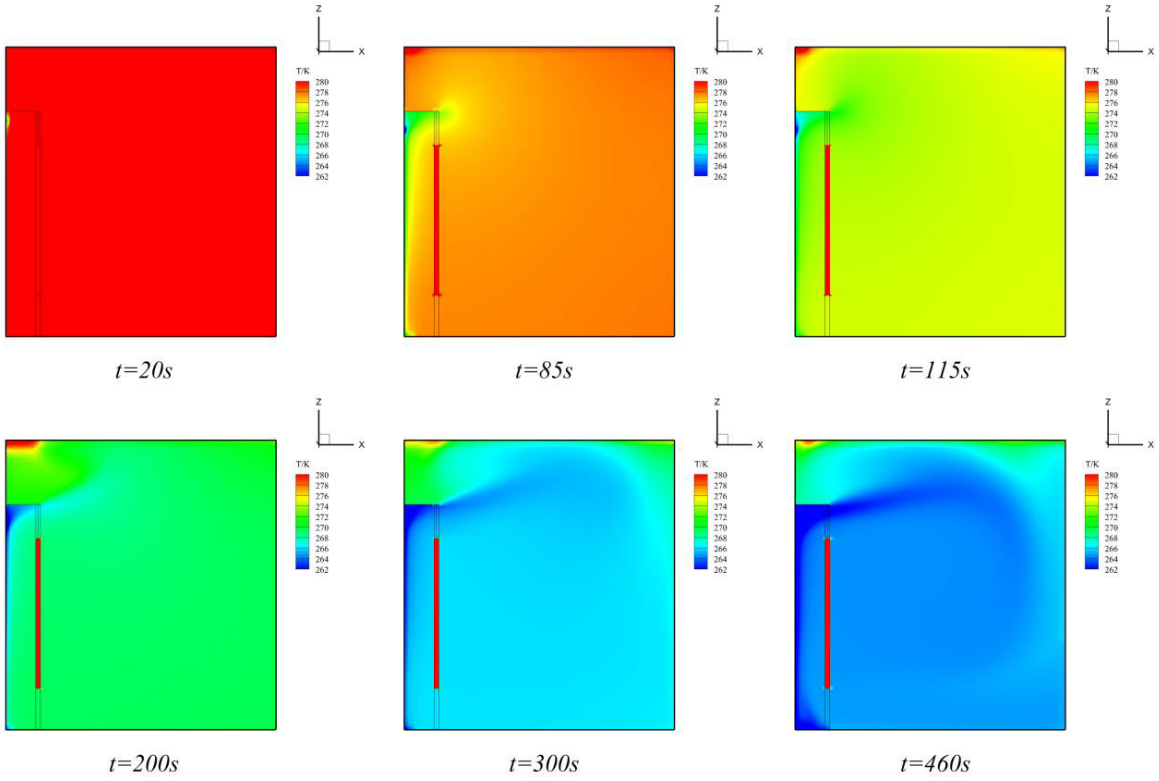

Fig 7 The evolution of temperature distribution from room temperature to －7℃

2.2 Stage from －7℃ to －5℃

Once the temperature of the storage room reaches －7℃, simulation is carried out and the refrigeration is switched off. When the refrigeration is switched off, the flow field is hardly affected. Then in the following we only present the evolution of the temperature distribution.

Fig 8 presents the evolution of the temperature distribution in the refrigeration cabinet during this period when the refrigerator is switched off. Due to the action of fan and the heat flux through both glass door and the cabinet walls, the temperature in the refrigeration compartment quickly equilibrates with the temperature in the storage compartment. Temperature in the refrigeration and storage compartments also increases gradually. In the storage room, there is still a region near the centre with relatively low temperature. The temperature in the cabinet eventually increases from －7℃ to －5℃ at about 30s (from t=460s in Fig 7 to t=490s in Fig 8).

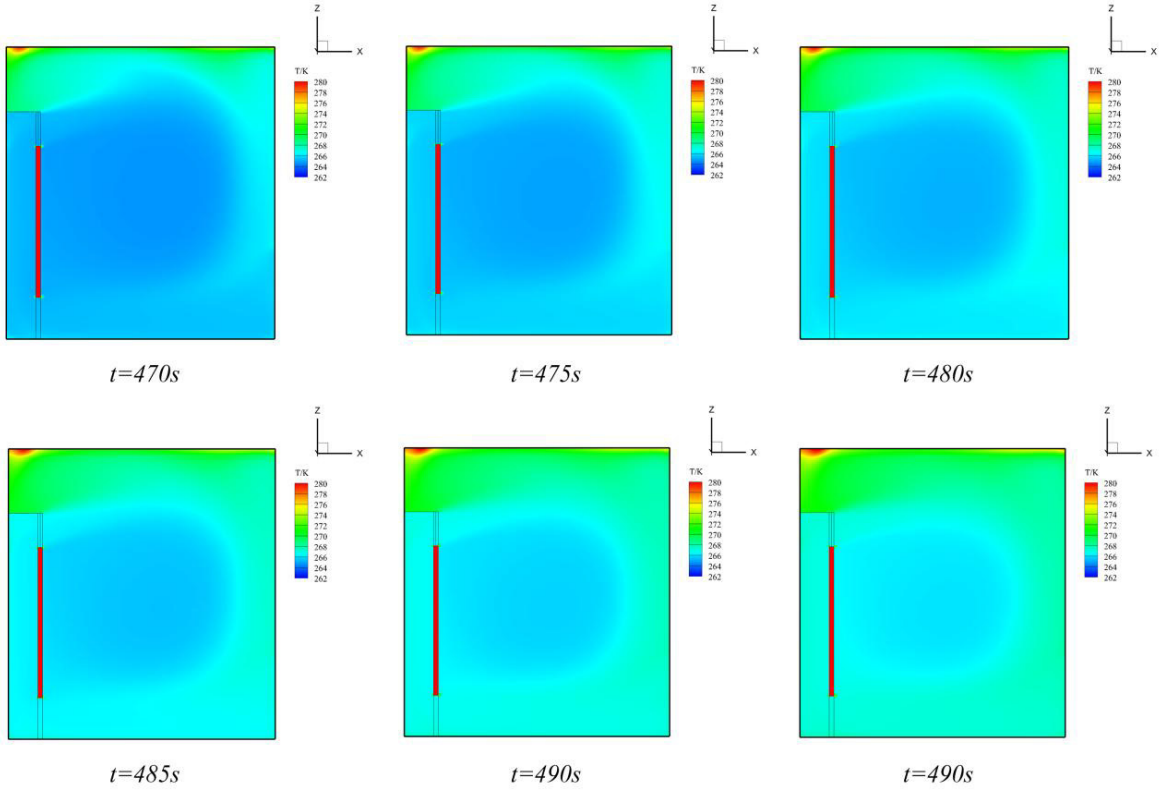

Fig 8 The evolution of temperature distribution from - 7℃ to - 5℃

2.3 Stage from - 5℃ to - 7℃

Once the temperature in the storage cabinet reaches - 5℃, simulation is carried out and the evaporator is switched on. Fig 9 presents the evolution of the temperature distribution during this period. When the evaporator is switched on again, the air in the refrigeration room is cooled and the lowest temperature appears near the evaporator. Subsequently, the cooled air passes through the upper perforated plate, and mixes with the air in the storage cabinet, resulting in the temperature in storage room decreased. During this process, the region near the glass door has a relatively high temperature and the relatively high temperature zone becomes small with time develops. Finally, the time required to cool the air in the cabinet from - 5℃ to - 7℃ is about 110s (from t=490s in Fig 8 to t=600s in Fig 9).

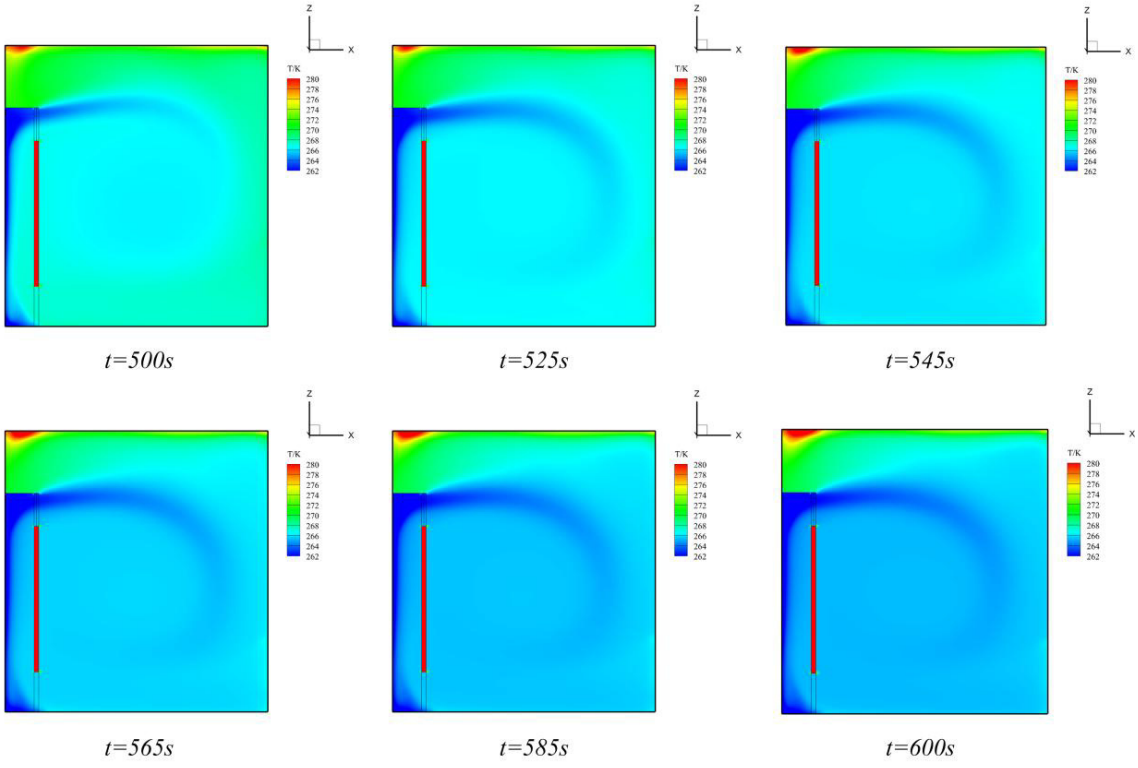

Fig 9 The evolution of temperature distribution from - 5℃ to - 7℃

Finally, we present the 3D flow field and the 3D temperature distribution of each stage at its end (see Fig 10(a) and Fig 10(b) respectively). From Fig 10(a) we can see that the 3D flow fields of each stage at its end are nearly the same when the air is fully developed under the action of fan. This is consistent with our recognition and is the reason why we do not present the evolution of flow field for the latter two stages in Sections 4.2 and 4.3. From Fig 10(b) we can see that the 3D temperature distributions of the first and third stages at their end for cooling products are almost the same, although some minor discrepancy emerges. In contrast, the 3D temperature distribution of the second stage at its end is obviously different with relatively high temperature.

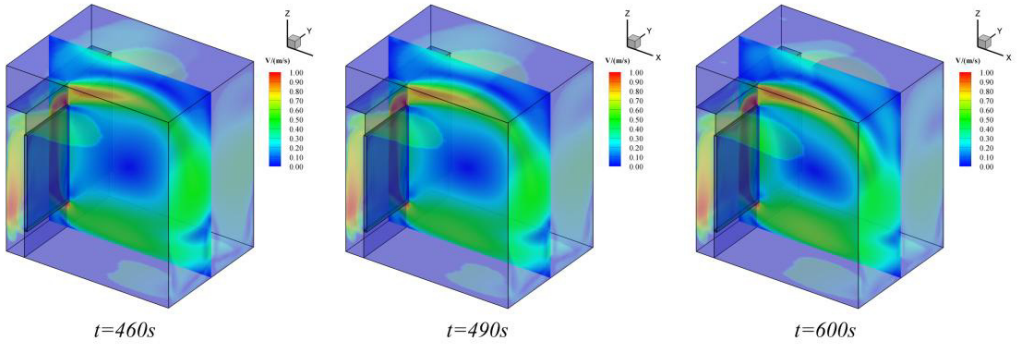

(a)

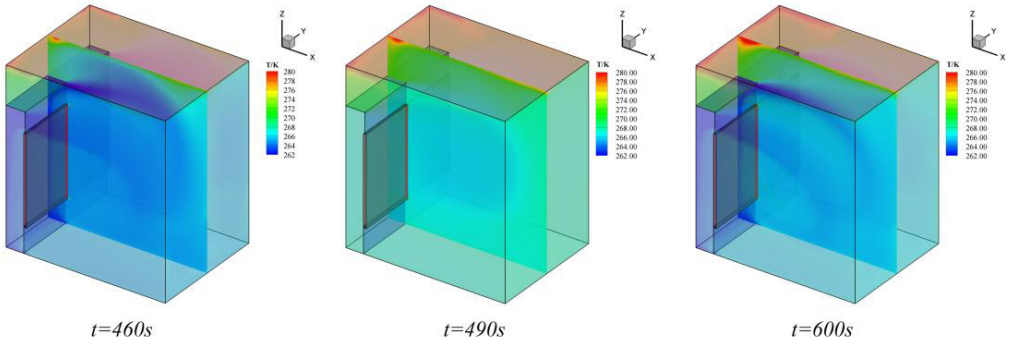

(b)

Fig10 The 3D picture of each stage at its end: (a) flow field, (b) temperature distribution

5. Conclusions

In this paper, commercial software Fluent has been used to build a 3D CFD model for dynamic study of air flow and heat transfer in refrigeration cabinet. The dynamic cycle of switching on and switching off has been simulated. The refrigeration cabinet is composed of an enclosed refrigeration compartment and a product storage compartment connected by perforated plate at the top and an opening slit at the bottom. The perforated plate is used to distribute the coolant air flow to ensure uniform mixing in the storage compartment.

To simulate the effect of perforated plate, the porous-jump model is used. The model is calibrated to a benchmark problem with one open channel whose area is equivalent to the total effective open area of the holes of the perforated plate. By matching the overall flux, the parameters in the porous-jump model are determined. The dynamic processes simulated include three stages, namely the stage of initial start-up from room temperature to －7℃, the stage of auto switching off when the cabinet temperature reaches －7℃ and the restart stage when the cabinet temperature reaches －5℃. We demonstrated that in order to realistically simulate air flow and heat transfer in refrigeration cabinet, it is necessary to fully integrate refrigeration cycle and complex boundary conditions including possible forced air circulation. Supercomputing in 3D is also necessary. In this way, our simulation results can be used to improve the performance of refrigeration cabinet with zero prototyping.

Acknowledgements

This work is financially supported by the Unilever under Grant No. CH-2010-0026, the National Natural Science Foundation of China under Grants No. 21106155 and the Chinese Academy of Sciences under Grant No. XDA07080303.

References

[1] R. Faramarzi, Efficient display case refrigeration, ASHRAE J, 1999(November) 46-54.
[2] D. Walker, V. Baxter, Analysis of advanced, low charge refrigeration for supermarkets, in: ASHRAE summer meeting, 2002.
[3] J. Moureh, G. Letang, B. Palvadeau, H. Boisson, Numerical and experimental investigations on the use of mist flow process in refrigerated display cabinets, International Journal of Refrigeration, 32 (2009) 203-219.
[4] S. Marinetti, G. Cavazzini, L. Fedele, F. Zan, P. Schiesaro, Air velocity distribution analysis in the air duct of a display cabinet by PIV technique, International Journal of Refrigeration, 35 (2012) 2312-2331.
[5] D. Yashar, H. Cho, P. Domanski, Measurement of air-velocity profiles for finned-tube heat exchangers using particle image velocimetry, in: International Refrigeration and Air Conditioning, Purdue University, 2008.
[6] Y. Chen, X. Yuan, Experimental study of the performance of single-band air curtains for a multi-deck refrigerated display cabinet, Journal of Food Engineering, 69 (2005) 261-267.
[7] B. Field, E. Loth, Entrainment of refrigerated air curtains down a wall, Experimental Thermal and Fluid Science, 30 (2006) 175-184.
[8] K. Yu, G. Ding, T. Chen, Experimental investigation on a vertical display cabinet with central air supply, Energy Conversion and Management, 50 (2009) 2257-2265.
[9] Y. Ge, S. Tassou, A. Hadawey, Simulation of multi-deck medium temperature display cabinets with the integration of CFD and cooling coil models, Applied Energy, 87 (2010) 3178-3188.
[10] A. Foster, M. Madge, J. Evans, The use of CFD to improve the performance of a chilled multi-deck retail display cabinet, International Journal of Refrigeration, 28 (2005) 698-705.
[11] G. Cortella, CFD-aided retail cabinets design, Computers and Electronics in Agriculture, 34 (2002) 43-66.
[12] G. Cortella, M. Manzan, G. Comini, CFD simulation of refrigerated display cabinets, International Journal of Refrigeration, 24 (2001) 250-260.
[13] Z. Cao, B. Gu, G. Mills, H. Han, A novel strategy for predicting the performance of open vertical refrigerated display cabinets based on the MTF model and ASVM algorithm, International Journal of Refrigeration, 33 (2010) 1413-1424.
[14] N. Smale, J. Moureh, G. Cortella, A review of numerical models of airflow in refrigerated food applicatoins, International Journal of Refrigeration, 29 (2006) 911-930.
[15] P. D'Agaro, G. Cortella, G. Croce, Two- and three-dimensional CFD applied to vertical display cabinets simulation, International Journal of Refrigeration, 29 (2006) 178-190.